Iran. J. Radiat. Res., 2005; 3 (3): 135-142

Improving the performance of neural network in differentiation of breast tumors using wavelet transformation on dynamic MRI

P. Abdolmaleki[1*], H. Abrishami-Moghddam[2], M. Gity[3], M. Mokhtari-Dizaji[4], A. Mostafa[2]

[1] Department of Biophysics, Tarbiat Modares University, Tehran, Iran
[2] Department of Electrical Engineering, K.N. Toosi Universiy of Technology, Tehran, Iran
[3] Department of Radiology, Imam Khomainei Hospital, Tehran University of Medical Sciences Tehran, Iran

Background: A computer aided diagnosis system was established using the wavelet transform and neural network to differentiate malignant from benign in a group of patients with histo-pathologically proved breast lesions based on the data derived independently from time-intensity profile. ***Materials and Methods:*** The performance of the artificial neural network (ANN) was evaluated using a database with 105 patients' records each of which consisted of 8 quantitative parameters mostly derived from time-intensity profile using wavelet transform. These findings were encoded as features for a three-layered neural network to predict the outcome of biopsy. The network was trained and tested using the jackknife method and its performance was then compared to that of the radiologists in terms of sensitivity, specificity and accuracy using receiver operating characteristic curve (ROC) analysis. ***Results:*** The network was able to classify correctly the 84 original cases and yielded a comparable diagnostic accuracy (80%), compared to that of the radiologist (85%) by performing a constructive association between extracted quantitative data and corresponding pathological results (r=0.63, p<0.001). ***Conclusion:*** An ANN supported by wavelet transform can be trained to differentiate malignant from benign breast tumors with a reasonable degree of accuracy. **Iran. J. Radiat. Res., 2005; 3 (3): 135-142**

Keywords: *MR Imaging, wavelet transform, neural network, Breast.*

INTRODUCTION

Breast cancer is the most prevalent cancer among women, and has become the leading cause of cancer deaths among women 15 to 54 years old[1]. The best way to reduce cancer deaths due to breast cancer is early detection and treatment. Currently, self-examination, mammography, and MRI are the most frequently adopted methods for early detection of breast cancers.

The ANN has been applied in breast cancer diagnosis using subjective impression of different features based on defined criteria[2, 3]. In the studies of Chen and colleagues, the benign and malignant tumors were classified using a 5×5 normalized auto correlation matrix and a multilayer feed-forward neural network[4]. Although it is widely showed of good performance, but some reports have shown some disadvantages such as: the presence of the inter- and intra-observer disagreement in features categorization, as well as final interpretation[5]. This variability causes an inconsistency in feature categorization as well as final diagnosis. Using such subjective data which strongly relies on the correctness of observer interpretation as input into the ANN sometimes make a confusable situation for ANN and therefore affect the performance of neural network[5]. Recently some reports suggested the possibility of using directly extracted quantitative features as input into the ANN in a few fields of radiology in which the quantitative data is accessible[5].

On the other hand, wavelet transform has been identified as a good technique for the representation of time-frequency signals. It has been applied in many image techniques, such as feature enhancement, texture discrimination, texture segmentation, pattern recognition, data compression, teleradiology and image acquisition[6-9]. Meanwhile, the distribution of wavelet coefficients can be utilized for differentiating

Corresponding author:
Dr. Parviz Abdolmaleki, Department of Biophysics, Faculty of Science, Tarbiat Modares University, Tehran. P.O. Box 14115-175, Iran.
Fax: *+98 21 88009730*
E-mail: *parviz@modares.ac.ir*

malignant cases from benign cases, because local texture characteristics are well reinforced by wavelet transform. The neural network is a model that simulates the human learning process. Recently, it has been applied in many discriminating systems with good performance, such as pattern recognition, voice recognition and optical character reading. In the researches of differentiating breast tumors, the neural network has also been successfully applied to detect microcalcifications in digital mammographic images[10-12].

In this study a computerized method was developed to extract quantitative features directly from computer generated time-intensity profiles using wavelet transform and analyzing them using an ANN. Our objectives in this study were: 1) to extract independent features directly from time-intensity profile using wavelet transform; 2) to minimize the reliance of the output of the ANN on the correctness of radiological interpretation which depends to the factors like the experience of the reader, time of reading and criteria used for extracting the data.

MATERIALS AND METHODS

Neural networks

We employed a three-layered, feed forward neural network with a back propagation algorithm for training. The network designed to distinguish benign and malignant on the basis of features that had been extracted from signal-intensity profile using wavelet transform. Our study group consisted of 105 female patients whose ages ranged from 15 to 79 years (mean 52 yrs). The patients group included 75 malignant lesions and 30 benign entities. The excision biopsy was performed for all patients (n= 105).

Data acquisition

MRI images

The MRI images were taken at the Imam Hospital Imaging Center and Athari Imaging Center during the 2002-2005 both using similar system of Signa 1.5 Tesla unit (GE Medical Systems, Milwaukee, Wis) in the prone position. The majority of cases were performed using a specific breast coil while the minority of cases were performed by a surface coil. Initial sagittal or axial T1-weighted spin-echo images (T1W) were performed at 325/8 (repetition time (msec)/echo time (msec)) and axial or sagittal T2-weighted fast spin-echo images (T2W) with or without fat suppression for tumor localization were performed at 5,400/90. Other MR parameters used were 22 cm field of view, 3.6 mm section thickness, and 256×192 (T1-weighted) or 256×256 (T2-weighted) matrix. Dynamic study was performed after administration of gadopentetate dimeglumine (Magnevist; Schering, Berlin, Germany) over 10-15 seconds using a fast radio-frequency spoiled gradient-recalled-echo (SPGR) sequence (11.4/3.3; flip angle,10 degree; matrix, 256×192; section thickness, 3.6 mm; gap, 1.0-2.5 mm). The dose of contrast agent was 0.2 ml/kg body weight which was 15 ml for a patient with 75kg weight. An automatic injector was used with a rate of injection of 1 ml/second over 10-15 seconds.

Feature generation

For the quantitative assessment, the images were called back one by one and a free size region of interest (ROI) were drawn in the most enhancing part of the lesion (figure 1). An ROI image is an appropriate image containing the important contents which we are interested in. The obtained time-intensity values were used to generate the time

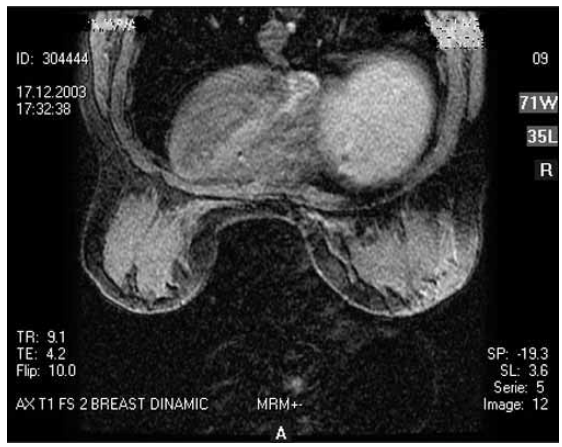

Figure 1. Free size ROI were drawn in the histogram showing average most enhancing part of the lesion.

intensity profile. A locally written program based on wavelet analysis was then applied to obtain the following features from the signal intensity profile:

1) The variance of the high frequency coefficients in the first scale of wavelet transform for the 5 early points of the signal in wash-in part of the signal intensity profile.
2) The variance of the high frequency coefficients in the second scale of wavelet transform for the 4 early points of the signal in wash-in part of the signal intensity profile.
3) The variance of the high frequency coefficients in the first scale of wavelet transform for the 6 last points of the signal in wash-out part of the signal intensity profile.
4) The variance of the high frequency coefficients in the second scale of wavelet transform for the 4 last points of the signal in wash-out part of the signal intensity profile.
5) The variance of the low frequency coefficients in the first scale of wavelet transform for the 6 last points of the signal in wash-out part of the signal intensity profile.
6) The variance of the low frequency coefficients in the second scale of wavelet transform for the 4 last points of the signal in wash-out part of the signal intensity profile.
7) The energy of the high frequency coefficients in the first scale of wavelet transform for the whole signal.
8) The energy of the high frequency coefficients in the second scale of wavelet transform for the whole signal.

A brief explanation for the wavelet transform was presented in the Appendix. These eight features were selected on the basis of their qualitative correlation with medical experience. Table 1 shows the parameters in our database, which represented all extracted features from the analyzing the signal-intensity profile using wavelet transformation. For the simulation of the neural network, all the quantitative data were normalized between 0 and 1 according to the maximum value of each feature in the data set. The normalized data was then feed forward into the network to

Table 1. The extracted quantitative parameters from time-intensity profile which used as input into the neural network.

	Indexes	Mean ± S.D.(×1.0e+003)	Range (×1.0e+003)
1	The VHFC* in the first scale of WT** for the 5 early points of the signal in wash-in part of the SI*** profile.	0.1648 ± 0.2393	1.260
2	The VHFC in the second scale of WT for the 4 early points of the signal in wash-in part of the SI profile.	1.0459± 1.3422	7.327
3	The VHFC in the first scale of WT for the 6 last points of the signal in wash-out part of the SI profile.	0.0267± 0.0475	0.3350
4	The VHFC in the second scale of WT for the 4 last points of the signal in wash-out part of the SI profile.	0.0219 ± 0.0361	0.1990
5	The VLFC**** in the first scale of WT for the 6 last points of the signal in wash-out part of the SI profile.	0.0269 ± 0.0455	0.2630
6	The VLFC in the second scale of WT for the 4 last points of the signal in wash-out part of the SI profile.	0.0296 ± 0.0627	0.4260
7	The energy of the high frequency coefficients in the first scale of WT for the whole signal.	0.9414 ± 1.2410	6.6620
8	The energy of the high frequency coefficients in the second scale of WT for the whole signal.	3.4182 ± 4.4968	27.7740

Note:
* Variance of the high frequency coefficients in the first scale
** Wavelet transformation
*** Signal intensity
**** Variance of the coefficient of the low frequency

map them with corresponding pathological findings.

Radiological assessment

One reader (MG) was then asked to read and report her findings from conventional pre and post contract T1 and T2-weighted images as well as dynamic images. Imaging findings were graded on the following features; size, shape, lesion margin, enhancement homogeneity, time-intensity profile type, as well as other associated features. The classification for the curve type has been performed as described by Buadu[14].

Neural networks structure

The neural network, which was employed in this study, had three layers. The first layer consisted of 8 input elements, each of which corresponded to data extracted from the wavelet analysis on signal intensity profile; the second layer, the hidden layer, had 5 nodes and finally the output layer with 1 element, which represented 1 for malignant and 0 for benign lesions. In order to determine the best optimized structure for the neural network, we simulated a large number of neural networks by varying the number of hidden nodes, iterations and learning rates.

Our network was trained and tested using the jackknife technique in which all cases were used in both the training and testing processes[15]. In this method, all but one case in the database was used to train the network. The single case that is left out is then used to test the network. This procedure was repeated until each case in the database is used once as a testing case.

Finally, after the network had been trained perfectly in each simulation the testing case was presented to the trained network giving a diagnostic output vector in the range of (0-1). Our network was trained perfectly over 200,000 iterations on a IBM compatible personal computer (Pentium III 800 MHz). The software used to construct the neural network was written locally in MATLAB programming language[16].

Performance evaluation

The sophisticated receiver operating characteristic ROC analysis was selected to evaluate the performance of neural network approach and that of radiologists[17]. After the network had been trained perfectly in each simulation the testing set was presented to the trained network giving a diagnostic output vector in the range of (0-1). The outputs of the testing set were then analyzed to determine the true-positive and the false-positive fractions, which were then used for plotting the ROC curves. The area under the ROC curve (A_z) was then used to compare the performance of ANN as well as the radiologist participating in the testing procedure.

To evaluate the performance of the observers, an expert reader (MG) was asked to record their findings into one of the five categories with increasing likelihood of malignancy; 1 (benign), 2 (probably benign), 3 (indeterminate), 4 (probably malignant), 5 (malignant). Similarly, to evaluate the performance of the neural network, the network output was classified into five categories; output in range of (0-0.2) = benign, (0.2- 0.4) = probably benign, (0.4-0.6) = indeterminate, (0.6-0.8) = probably malignant and output in range of (0.8-1) = malignant.

RESULTS

The experimental results and performance evaluation of the proposed method are described in this section.

Radiologist performance

One expert reviewer with high level of experience read the images and classified them into benign and malignant groups using a five-scale category with increasing likelihood of malignancy. The participated radiologists could reach to diagnostic accuracy of 85% by making correct classifications for 68 of 75 patients with malignant breast cancers and 21 of 30 with benign entity. This yielded to a remarkable sensitivity of 91% as well as a moderate specificity of 70%.

Neural network performanc

The output of neural network showed a correct classification for 65 of 75 patients

with malignant breast cancers and 19 of 30 with benign entity. This yielded a diagnostic accuracy (80%) for the ANN, which is comparable to the average outcomes obtained for the high experienced radiologists (85%). Table 2 summarizes the average results obtained for the participating radiologist compared with the prediction of neural network in terms of sensitivity, specificity, accuracy, false positive, false negative, misclassified rate.

Table 2. Comparative performance of ANN and participating radiologists.

Parameter	Participating expert radiologist	Artificial neural network
Sensitivity (%)	91	87
Specificity (%)	70	63
Accuracy (%)	85	80
False positive fraction	9 of 30	11 of 30
False negative fraction	7 of 75	10 of 75
No. of cases with misdiagnosis	16	21
Misclassified rate (%)	15	20

We also applied ROC analysis to our data to confirm the obtained results. Using the best results obtained for the radiologist as well as the ANN, an ROC analysis was also performed. The area under the receiver operating characteristic curves (A_z) for the ANN was A_z (net) = 0.7584 ± 0.0581, with an accuracy of 80%, for the participated radiologist A_z (doc) = 0.7980±0.0569, with a maximum of 85% accuracy. Figure 2 illustrates the ROC curves for different schemes in the classification of malignant and benign tumors.

DISCUSSION

Despite the existence of many kinds of detection methodologies, the best way is biopsy to differentiate whether the tumor accurately is benign or malignant. In comparison with other procedures, biopsy is a very expensive procedure for the large number of indeterminate lesions that need to

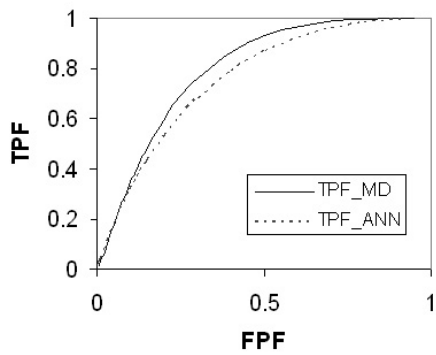

Figure 2. Resulting receiver operating characteristic curve comparing the diagnostic performance of the neural network with that of the radiologist. The "ANN" and "MD" are referring to the neural network and the participated radiologist.

be differentiated per tear[18]. Therefore, it becomes constructive to diminish invasive methods of distinguishing malignant from benign masses of the breast to reduce the number of unnecessary biopsies. In this study we assumed that applying the quantitative parameters extracted by wavelet transform from the time intensity profile and analyzed by an ANN program can possibly reduce the present overlap between the benign and malignant patterns. This assumption is justified because the previous report suggested the ability of the wavelet transform to separate frequency components of the signal and represent them as a function of time [13, 19]. In other words, wavelet transform of the signal intensity profile is a 2D map representing frequency components of the signal in different time intervals [13, 20]. This can somehow explain the phase of the trace of contrast medium in wash-in and wash-out part of bolus injection. To achieve this purpose, we analyzed the temporal progression of contrast enhancement by plotting the rate of change of signal intensity as a function of time. In addition, we analyzed the time intensity profiles basing it on the peak enhancement and wash-out of the contrast medium. In this regard the two first parameters which somehow represent the gradient of the steepest part of the contrast uptake curve were then included. This feature selection is justified because it is reported that the presence of the sharp enhancement especially during the early phase (within 120 seconds after the bolus injection) has a strong correlation with the

histopathologic findings[14, 21]. Also the features 3 to 6 were included, because they represented the change of the contrast enhancement in the wash-out part of signal intensity profile; moreover, features 7 and 8 are used to represent overall distortions of the measured signals. These features could have a normalization effect on the other 6 features. That means if a defined signal is very oscillating, its energy features [7, 8] will be larger and the gradient measures in features 1 to 6 will be normalized by these larger energy values. Among the too many available independent quantitative parameters we selected those with some similarities with the contrast enhancement as input into the ANN [22, 23]. The previous reports suggested the great power of the ANN in associating too many independent linear and/or nonlinear parameters. This happened by establishing similarities between evaluated parameters in the training set during the training process by addressing them as proportional weights. These defined weights were then used during the testing process to evaluate the degree of malignancy for the cases that have not been previously presented to the computer. In this regard, we applied our program to a population of patients with proven histo-pathological findings to predict the outcome of biopsy based on the quantitative data extracted directly from signal intensity profile using wavelet transform. Using such objective quantitative data, our network was trained and tested by the conventional round rubbin method on 105 proven cases. Our goals were to reduce the number of benign cases sent to biopsy using neural network as a supportive tool based on data extracted from time intensity profiles using wavelet transform. By doing so, we eliminate the reliance of the output of the ANN on the correctness of radiological interpretation which it is depend to the factors like the experience of the reader, time of reading and criteria used for extracting the data.

Vomweg and coworkers developed an ANN in conjunction with a computer program for input variable selection to differentiate the benign and malignant patterns using the quantitative data extracted from the contrast-enhanced magnetic resonance-mammography in 604 histologically proven cases[24]. They reported that their ANN achieved a sensitivity of 93.6% and a specificity of 91.9% in predicting malignancy of lesions within an independent prediction sample set while the participated expert radiologist was worse than the ANN (sensitivity 92.1%, specificity 85.6%). Similarly, Szabo and coworkers recently introduced a minimized ANN based model in a dataset of 89 women with 105 histopathologically verified breast lesions using dynamic MR imaging features of the breast. They compared ANN model with the performance of a human reader using the area under the ROC curve. These authors indicated that the performance of the ANN (A_z = 0.771) is comparable to the result obtained for the expert radiologist (A_z = 0.799). Using the same prediction scale, the minimized ANN model performed best followed by the best kinetic (A_z = 0.743), the maximized (A_z = 0.727), and the morphologic model (A_z = 0.678). The performance of a neural network prediction model is comparable to that of an expert radiologist[25]. Our obtained results (indicating comparable results to the expert) support the above mentioned reports by highlighting the potential usefulness of the applying ANN in breast cancer diagnosis.

Ultimately, the overall average results for sensitivity, specificity, and accuracy of 87%, 63%, and 80% for the ANN were comparable with those obtained for participated expert radiologist: 91%, 70%, and 85%. This indicates that a three-layer feed-forward neural network jointed with a preprocessor in the form of wavelet transform can be trained to successfully support radiologists in differentiating malignant from benign breast tumors. The moderate obtained of the low specificity may prove the previous report suggesting that the apparent overlap may be due to an inherent biological overlap[26]. Instead of immediate biopsy after abnormal screening, these results suggest that women would find non-invasive triage tests acceptable, or preferable to biopsy if they were equally accurate or nearly equally accurate as a biopsy. New technologies to

diagnosis breast cancer should focus on decreasing discomfort as well as increasing accuracy.

ACKNOWLEDGMENT

The authors are indebted to Miss Akram Pakniat for her valuable assistance in collecting the data.

Appendix

A brief theory of Wavelet transform

The wavelet transform can be regarded as a signal expansion using a set of basis functions, which are obtained from a single prototype function $\psi(x)$, called *Mother Wavelet*. By definition a function $\psi(x)$ can be considered to be mother wavelet if [13]

$$\int_{-\infty}^{\infty} \psi(x)dx = \Psi(0) = 0 \qquad (1)$$

Where $\Psi(\omega)$ is the Fourier transform of the function $\psi(x)$. The wavelet transform of a 1D real function $f(x) \in L^2(R)$ with respect to a mother wavelet $\psi(x)$ is defined as

$$W(s,t) = \frac{1}{\sqrt{|s|}} \int_{-\infty}^{\infty} f(x)\psi\left(\frac{x-t}{s}\right)dx \qquad (2)$$

The wavelet transform $W(s,t)$ gives a scale-space decomposition of the signal $f(x)$ with s indexing the scale and t indexing position in the original signal space. In practice, the wavelet transform scale and translation parameters are discretized and for fast numerical implementation the scale normally varies along a dyadic sequence. This yields the *Discrete Dyadic Wavelet Transform:*

$$W(j,n) = 2^{-j/2} \int_{-\infty}^{\infty} f(x)\psi(2^{-j}(x-n))\,dx \qquad (3)$$

For a discrete signal of length N, the maximum number of available scales is defined as $J = \log_2(n) + 1$. Figure 3 shows wavelet decompositions in two levels using Daubechies wavelets. In figure 3-a, wavelet coefficients corresponding to a benign case signal is illustrated. Wavelet decomposition of a malignant case signal is shown in figure 3-b. In this figures no sub-sampling has been applied.

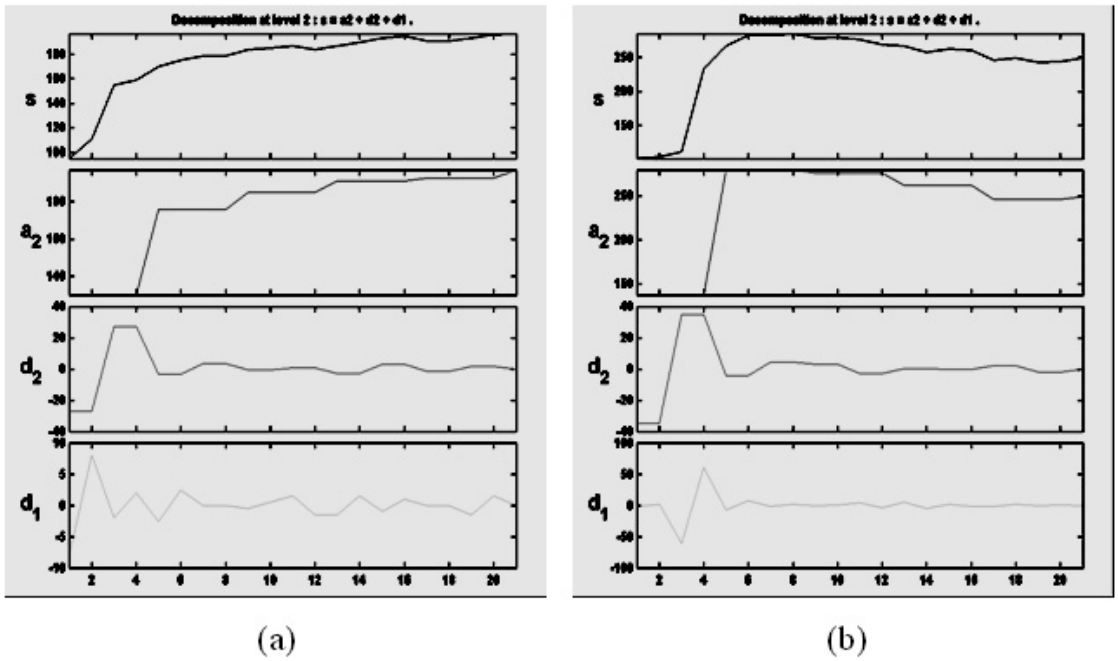

Figure 3. Two level wavelet decomposition using Daubechies wavelets of (a) benign and (b) malignant signals. No subsampling has been applied.

REFERENCES

1. Chen DR, chang RF, Kuo WJ, Chen MC, Huang YL (2002) Diagnosis using wavelet transform and neural networks. *Ultrasound Med Biol,* ***28:*** *1301-1310.*
2. Hollingsworth AB, Stough RG (2003) The emerging role of breast magnetic resonance imaging. *J Okla State Med Assoc,* ***96:*** *299-307.*
3. Peek ME (2003) Screening mammography in the elderly: a review of the issues. *J Am Med Women Assoc,* ***58:*** *191-8.*
4. Chen DR, Chang RF, Huang YL (1999) Computer aided diagnosis applied to US of solid breast nodules by using neural network. *Radiol,* ***213:*** *407-412.*
5. Elmore JG, Nakano CY, Koepsell TD (2003) International variation in screening mammography interpretations in community-based programs. *J Natl Cancer Inst,* ***95:*** *1384-93.*
6. Richardson WB (1995) Applying wavelet to mammogrms. *IEEE Eng Med Biol Mag,* ***14:*** *551-560.*
7. Kallergi M (2004) Computer-aided diagnosis of mammographic microcalcification clusters. *Med Phys,* ***31:*** *314-26.*
8. Papadopoulos A, Fotiadis DI, Likas A (2002) An automatic microcalcification detection system based on a hybrid neural network classifier. *Artif Intell Med,* ***25:*** *149-67.*
9. Gurcan MN, Chan HP, Sahiner B, Hadjiiski L, Petrick N, Helvie MA (2002) Optimal neural network architecture selection: improvement in computerized detection of microcalcifications. *Acad Radiol,* ***9:*** *420-9.*
10. Kocsis O, Costaridou L, Varaki L, Likaki E, Kalogeropoulou C, Skiadopoulos S, Panayiotakis G (2003) Visually lossless threshold determination for microcalcification detection in wavelet compressed mammograms. *Eur Radiol,* ***13:*** *2390-6.*
11. Penedo M, Pearlman WA, Tahoces PG, Souto M, Vidal JJ (2003) Region-based wavelet coding methods for digital mammography. *IEEE Trans Med Imaging,* ***22:*** *1288-96.*
12. Alterson R, Plewes DB (2003) Bilateral symmetry analysis of breast MRI. *Phys Med Biol,* ***48:*** *3431-43.*
13. Mallat SG (1999) A wavelet tour of signal processing. Academic Press, 2nd edition.
14. Buadu LD, Murakami J, Murayama S (1996) Breast lesions: correlation of contrast medium enhancement patterns on MR images with histopathologic findings and tumor angiogenesis. *Radiol,* ***203:*** *639-649.*
15. Tourassi GD, Floyd CE, Sostman HD, Coleman RE (1993) An artificial neural network approach for the diagnosis of acute pulmonary embolism. *Radiol,* ***189:*** *555-8.*
16. MATLAB user's guide (2002) The Math Works Inc, Mass.
17. Metz CE (1989) Some practical issues of experimental design and data analysis in radiological ROC studies. *Invest Radiol,* ***24:*** *234-245.*
18. Szabo BK, Wiberg MK, Bone B, Aspelin P (2004) Application of artificial neural networks to the analysis of dynamic MR imaging features of the breast. *Eur Radiol,* ***14:*** *1217-25.*
19. Behrenbruch CP, Marias K, Armitage PA, Yam M, Moore N, English RE, Clarke J, Brady M (2003) Fusion of contrast-enhanced breast MR and mammographic imaging data. *Med Image Anal,* ***7:*** *311-40.*
20. Alterson R, Plewes DB. (2003) Bilateral symmetry analysis of breast MRI. *Phys Med Biol,* ***48:*** *3431-43.*
21. Ivanovic V, Todorovic-Rakovic N, Demajo M (2003) Elevated plasma levels of transforming growth factor-beta 1 (TGF-beta 1) in patients with advanced breast cancer: association with disease progression. *Eur J Cancer,* ***39:*** *454-461.*
22. Vomweg TW, Buscema M, Kauczor HU, Teifke A, Intraligi M, Terzi S, Heussel CP, Achenbach T, Rieker O, Mayer D, Thelen M. (2003) Improved artificial neural networks in prediction of malignancy of lesions in contrast-enhanced MR-mammography. *Med Phys,* ***30:*** *2350-9.*
23. Vergnaghi D, Monti A, Setti E, Musumeci RA (2001) Use of a neural network to evaluate contrast enhancement curves in breast magnetic resonance images. *J Digit Imaging,* ***14:*** *58-9.*
24. Vomweg TW, Buscema M, Kauczor HU, Teifke A, Intraligi M, Terzi S, Heussel CP, Achenbach T, Rieker O, Mayer D, Thelen M (2003) Improved artificial neural networks in prediction of malignancy of lesions in contrast-enhanced MR-mammography. *Med Phys,* ***30:*** *2350-2359.*
25. Szabo BK, Wiberg MK, Bone B, Aspelin P (2004) Application of artificial neural networks to the analysis of dynamic MR imaging features of the breast. *Eur Radiol,* ***14:*** *1217-1225.*
26. Fobben ES, Rubin CZ, Kalisher L, Dembner AG, Seltzer MH, Santoro EJ (1995) Breast MR imaging with commercially available techniques: radiologic-pathologic correlation. *Radiol,* ***196:*** *143-152.*